INTERNATIONAL JOURNAL OF INTEGRATED ENGINEERING
ISSN: 2229-838X e-ISSN: 2600-7916

IJIE

Vol. 16 No. 7 (2024) 72-82
https://publisher.uthm.edu.my/ojs/index.php/ijie

A Cascaded Synchronous Buck Converter for Light Electric Vehicle Charging Applications

Mohammad Faisal Akhtar[1], Siti Rohani Sheikh Raihan[1], Nasrudin Abdul Rahim[1], Mohd Khairil Rahmat[2]*

[1] *Higher Institution Centre of Excellence (HICoE), UM Power Energy Dedicated Advanced Centre (UMPEDAC), Level 4, Wisma R&D, University of Malaya, Jalan Pantai Baharu, Kuala Lumpur 59990, MALAYSIA*

[2] *Electrical Engineering Section, British Malaysian Institute, Universiti Kuala Lumpur (UniKL), Batu 8, Jln Sg. Pusu, 53100 Gombak, Selangor, MALAYSIA*

*Corresponding Author: mkhairil@unikl.edu.my
DOI: https://doi.org/10.30880/ijie.2024.16.07.007

Article Info

Received: 25 June 2024
Accepted: 10 September 2024
Available online: 2 December 2024

Keywords

Light electric vehicle, synchronous DC-DC converter, non-isolated DC-DC converter, constant current, constant voltage

Abstract

In this work, a cascaded synchronous DC-DC converter topology is presented which is suitable for high current applications. In this topology, a synchronous buck converter is cascaded with a series capacitor synchronous buck converter, which exhibits very low step-down voltage gain – thus translating to a high current gain. For this work, this converter is applied for charging a 24 V, 10 A h Lithium-ion (Li-ion) battery. The constant-current constant-voltage (CC/CV) technique is employed with the proposed converter for this application. Simulations for the system were carried out in MATLAB Simulink, using the SimPowerSystems toolbox. The converter operation is observed to align with a typical CC/CV charging profile, with a 93.3% charging efficiency. Consequently, this topology may be integrated into an off-board charger for light electric vehicles (LEVs) such as e-bikes and three-wheeler e-rickshaws – which are typically used in public transportation. Suitability of the given converter is further corroborated by the observed charging efficiency. This work can potentially aim to address the issue of downtime that drivers of electric three-wheelers may face during peak operating hours. Consequently, this can open doors for further adoption of light electric vehicles for public transportation.

1. Introduction

The usage of fossil fuels in internal combustion engine (ICE) based vehicles has contributed greatly to the deterioration of the environment in recent years. As a consequence of this, electric vehicles (EVs) have emerged as a promising mode of transportation. As per the Stated Policies scenario described in the Global EV Outlook report compiled by the International Energy Agency (IEA) [1], around 16.5 million EVs were found worldwide at the end of 2021. As per the same report, EV sales globally are projected to grow up to 200 million by 2030. This goes on to show how there has been a growth spurt in EV usage over the past few years.

One specific segment – namely two/three-wheeler light electric vehicles (LEVs) – has seen potential for vast deployment in recent years, especially in developing urban areas. LEVs exhibit a compact design, have simple battery/charging requirements, and can be deployed for public transportation with ease. There are numerous examples in recent years which underline the popularity of LEVs: Compressed Natural Gas (CNG) based autorickshaws have largely taken a backseat to three-wheeler e-rickshaws [2]. Another example is of the usage

electric two-wheelers in Netherlands [3]. LEV sales growth in different regions in the 2019-2021 period is shown in Fig. 1 [1]. The upward trend in sales can be clearly observed, especially in Asian countries.

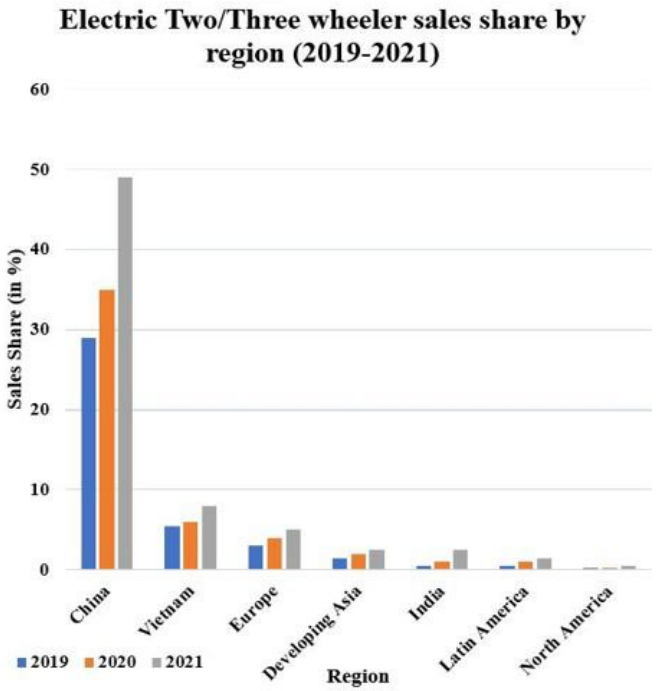

Fig. 1 *Electric two/three-wheeler sales growth by region [1]*

This rising number of LEVs on roads make it necessary that their charging systems be made more robust and widespread. A residential AC power supply is found to be enough for charging LEVs – facilitated by on-board chargers. These chargers convert the input AC supply into DC with the help of a power factor correction (PFC) stage, with another DC-DC converter being used for charging control [4]. Despite its easy availability, there exist drawbacks such as degraded power quality at the supply end, and an increased number of conversion stages which may hamper efficiency – owing to the PFC stage. Consequently, DC charging for LEVs has emerged as an alternative, akin to conventional EVs [5]. This method is characterized by the elimination of the dedicated AC-DC conversion stage, leading to an improved charging efficiency. Off-board charging stations are a possible means for carrying out DC charging, and this can also result in LEVs becoming more compact.

High-current gain DC-DC converters can be utilized for DC charging of LEVs for a more efficient charging process. These converters demonstrate a low step-down voltage gain, which translates to a high output current. Numerous applications such as communication systems and computer switch mode power supplies [6], [7] have reported usage of high current DC-DC converters. These converters can be broadly classified into: (a) isolated and (b) non-isolated DC-DC converters. High frequency transformers are typically used in isolated DC-DC converter topologies to achieve low step-down voltage gains, and hence a high current gain [8]. While this is a straightforward way to achieve this objective, these topologies suffer from a high component count, which becomes necessary to counteract the effects of transformer leakage inductance [9]. Furthermore, they are also relatively bulky due to the presence of the transformer.

Non-isolated converters have been proposed as an alternative for achieving high current gain [11-16]. The required voltage gain is not as straightforward to attain compared to isolated topologies, but it can still be done by using switched capacitors or coupled inductors [11], [12], which are still relatively more compact than a high frequency transformer. In [11], the authors presented a switched capacitor voltage quadrupler DC-DC converter, which utilized the charging and discharging action of capacitors to enhance the voltage gain. This topology possessed advantages such as high current gain, but a common ground between the supply and load was absent, which may result in susceptibility to electromagnetic interference (EMI). A cascaded DC-DC converter was proposed in [13], which delivered a high current gain. However, the topology had from high component count. Authors of [14], [15] presented quadratic DC-DC converter topologies which exhibited a very low voltage gain, while also having a common ground between the supply and load. An extendable topology was described in [14], which allowed for even lower even smaller step-down voltage gains. Lai et al [16] presented a series capacitor DC-DC converter having an interleaved structure at the output end, with a cascaded unregulated level converter stage. Reduced current ripples at the output end were observed owing to the interleaved structure. However, a high switch count was observed in the given circuit.

Int. Journal of Integrated Engineering Vol. 16 No. 7 (2024) p. 72-82

A good charging control technique is also equally important. It must effectively complement the chosen topology, and it must deliver optimal charging performance without causing battery damage. Taking this into consideration, the constant-current constant-voltage (CC/CV) technique [17] is chosen, as it remains popular in numerous charging applications. In this method, the charging current is held at a set point until the battery voltage reaches its maximum value. Beyond that point, the voltage remains fixed and the current steadily decreases.

In this study, cascaded DC-DC converter topology –combination of a synchronous buck converter and a series capacitor synchronous buck converter [9] – is presented. The proposed converter is advantageous for it's (a) relatively simple design and control and (b) higher current gain. The SimPowerSystems toolbox in MATLAB Simulink is used for analyzing the proposed converter's charging performance. A 24 V, 10 A h Lithium-ion battery is considered for this study. This work's main contributions are listed below:

- Demonstration of an enhanced current gain in DC-DC converters, as compared to other contemporary reported works.
- Demonstration of good efficiency in battery charging applications, thus proving that cascaded DC-DC converters can be viable for battery charging applications.

2. Proposed Topology

The proposed cascaded DC-DC converter is described in Fig.2. A synchronous buck converter – interfacing with the high voltage side – is cascaded with a series capacitor synchronous buck converter – interfacing with the low voltage side. The series capacitor C_B provides voltage divider characteristics to the given topology. Both converters are connected via an interfacing capacitor C_M.

The synchronous buck converter comprises of switches Q_1 and Q_2. It is a variation of the conventional buck converter, wherein a switch is used to replace the low side diode. This results in reduced voltage drop [18], thus resulting in an efficient performance, especially at large loads. The simplicity of this circuit has led it to become heavily used in consumer electronics [19], and it is this simplicity – alongside a relatively low number of switches – that has led to choosing the given circuit for the proposed topology.

The series capacitor synchronous buck converter comprises an interleaved stage of switches Q_1 and Q_2 along with inductors L_1 and L_2 respectively. Additionally, a series capacitor C_B is also present in the circuit, which contributes to the voltage divider. The advantages of this converter include (a) reduced passive component size owing to interleaving structure and (b) a voltage conversion ratio which is half that of a conventional buck converter. The synchronous series capacitor buck converter offers the combined benefits of switched capacitor topologies and interleaved buck converter topologies [20]. Considering these advantages, the series capacitor synchronous DC-DC converter is chosen as the low voltage side converter in this study.

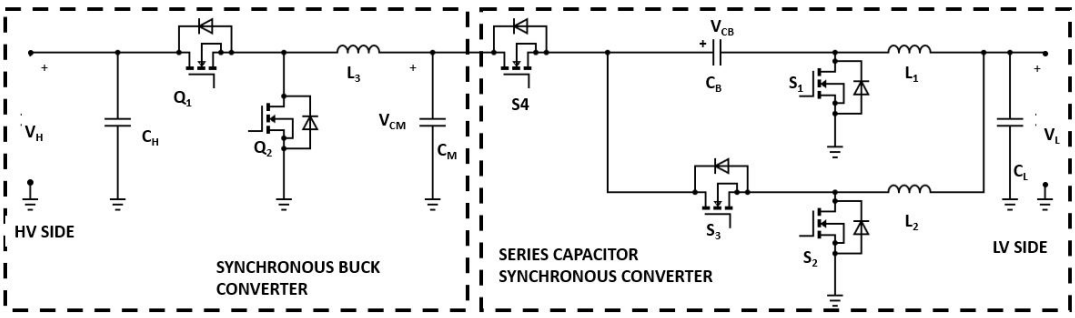

Fig. 2 *Proposed topology*

In this topology, switches {S_4, Q_1} and {S_1, Q_2} operate as main switch and synchronous rectifier respectively. Switches {S_3, S_2} operate complementarily compared to {S_4, S_1}. Additionally, it is to be noted that switches S_4 and S_3 operated 180 degrees apart, in a manner similar to interleaved converters.

2.1 Operating Principles

The step-down operation of the proposed converter comprises of four modes as shown in the waveforms in Fig. 3(a). Likewise, the corresponding states of the circuit are shown in Fig. 3(b). The capacitors are assumed to be large such that their voltage variations are negligible, and it is also assumed that the inductance of inductors L_1 & L_2 equal. Furthermore, D_b is the duty cycle of the switch and T_s is the time period for switching.

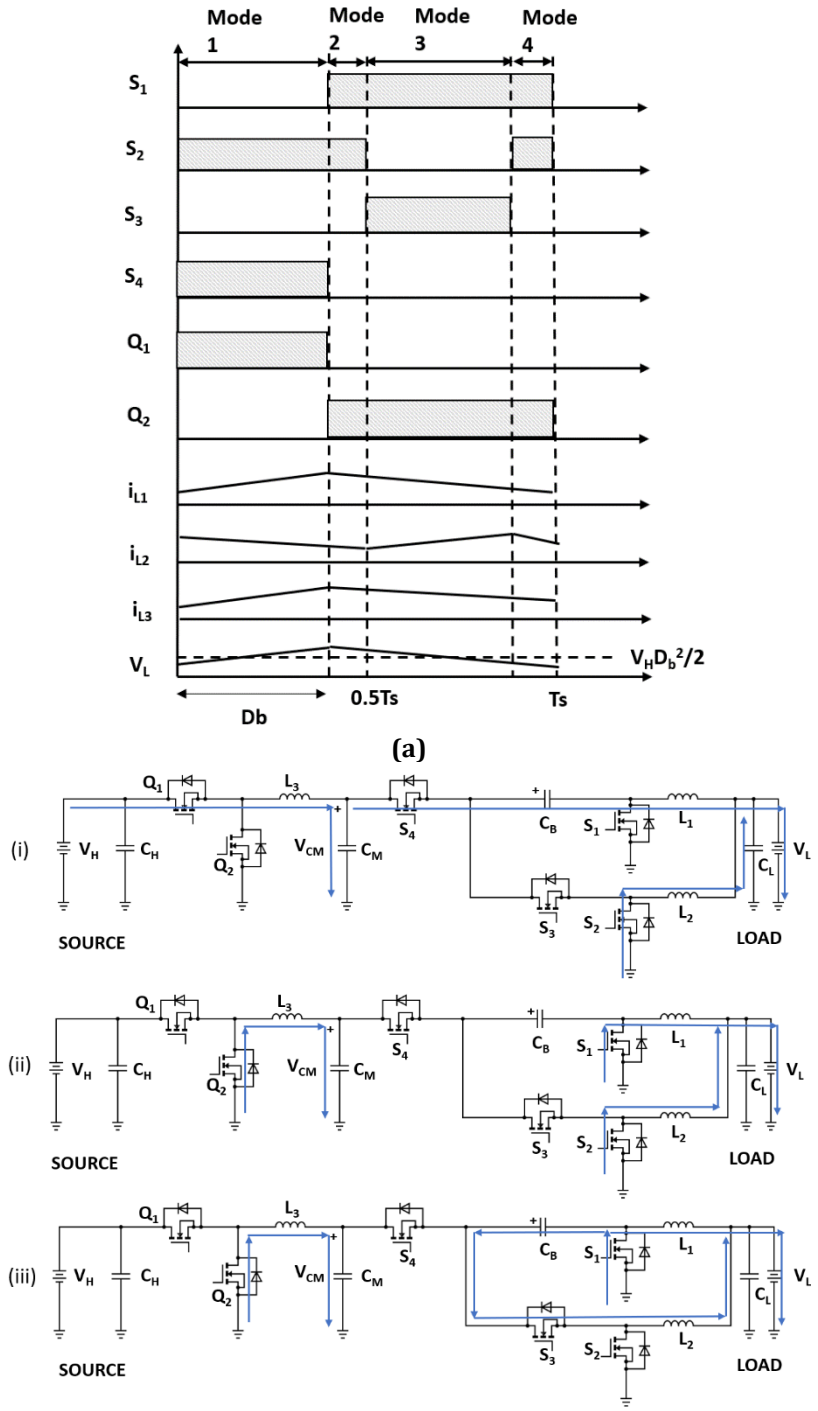

Fig. 3 *(a) Waveforms for the switching functions, inductor currents, and the output voltage during the four modes; (b) Circuit operation corresponding to (i) Mode 1 (ii) Mode 2 and 4 and (iii) Mode 3.*

- Mode 1 ($0<t<t_1$; duration = $D_bT_s = t_{ON}$): Switches S_4, Q_1 and S_2 are in conduction mode. The current through inductors L_1 and L_2 decrease. The current through inductor L_3 increases. Also, capacitor C_M directly feeds the load. The equations for the inductor currents are as shown.

$$L_1 \frac{di_{L1}}{dt} = V_{CM} - V_{CB} - V_L \tag{1a}$$

$$L_2 \frac{di_{L2}}{dt} = -V_L \tag{1b}$$

Int. Journal of Integrated Engineering Vol. 16 No. 7 (2024) p. 72-82

$$L_3 \frac{di_{L3}}{dt} = V_H - V_{CM} \quad (1c)$$

- Mode 2 ($t_1<t<t_2$; interval = $(0.5-D_b)T_s$): Current freewheels through inductors L_1 and L_2 and are decreasing. The load is fed through the energy stored in capacitor C_L. Switches S_1 and S_2 are ON. The switch Q_2 is ON, resulting in current decreasing through inductor L_3. The equations for inductor voltages are as shown.
-

$$L_1 \frac{di_{L1}}{dt} = -V_L \quad (2a)$$

$$L_2 \frac{di_{L2}}{dt} = -V_L \quad (2b)$$

$$L_3 \frac{di_{L3}}{dt} = -V_{CM} \quad (2c)$$

- Mode 3 ($t_2<t<t_3$; interval = D_bT_s): Switches S_1 and S_3 are ON, which results in increasing current through inductor L_2. Current through inductor L_1 reduces. Furthermore, Q_2 continues in ON state, and current through inductor L_3 decreases. Given below are the inductor voltages.
-

$$L_1 \frac{di_{L1}}{dt} = -V_L \quad (3a)$$

$$L_2 \frac{di_{L2}}{dt} = V_{CB} - V_L \quad (3b)$$

$$L_3 \frac{di_{L3}}{dt} = -V_{CM} \quad (3c)$$

- Mode 4 ($t_3<t<t_4$; duration = $(0.5-D_b)T_s$): This mode the same as to mode 2, with capacitor C_L feeding the load. Similar to modes 2 and 3, switch Q_2 continues to remain ON.

2.2 Derivation of Step-Down Gain

Consider $t_{ON} = D_bT_s$ to be the turn-on time of switches Q_4 and Q_3 and t_{OFF} to be their turn-off times. Recognizing that the inductor turn-on and turn-off current ripples are the same, we obtain the following expressions – while also referring to equations (1) through (3).

$$(V_{CM} - V_{CB} - V_L)\, t_{ON} - V_L t_{OFF} = 0 \quad (4)$$

$$(V_{CB} - V_L)\, t_{ON} - V_L t_{OFF} = 0 \quad (5)$$

From equations (4) and (5), we obtain the following expression for the series capacitor voltage V_{CB}.

$$V_{CB} = \frac{V_{CM}}{2} \quad (6)$$

This result proves that the series capacitor C_B is held at a constant voltage of $V_{CM}/2$. This acts as the additional capacitor voltage that contributes to voltage step-down gain as will be seen subsequently.
Using equations (1) through (3) and the result obtained in (6), volt-second balance is applied to obtain the step-down voltage gain as shown.

$$\frac{V_L}{V_{CM}} = \frac{D_b}{2} \quad (7)$$

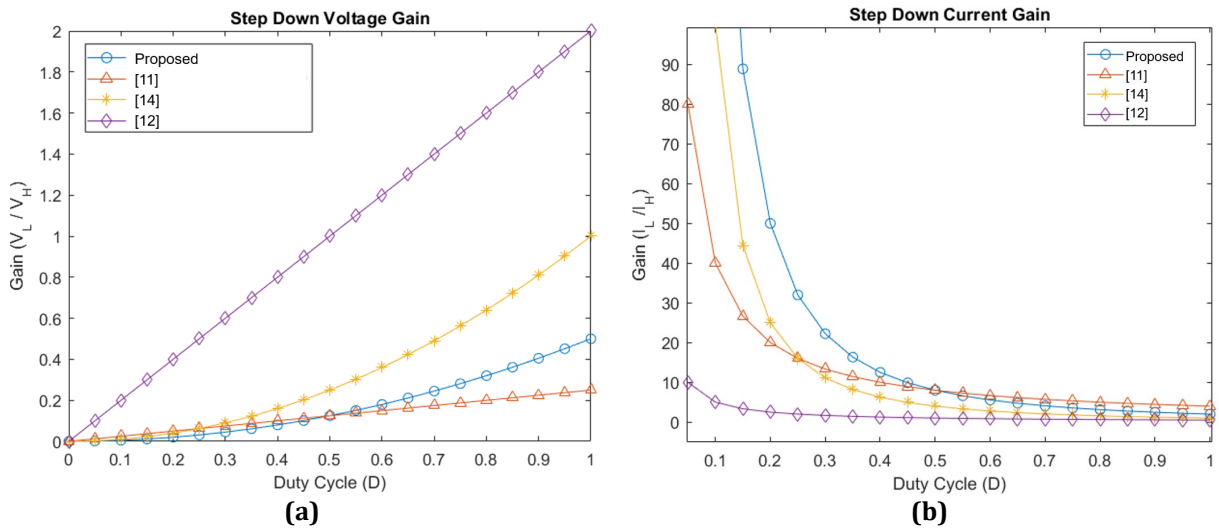

Fig. 4 *Proposed converter compared with other contemporary works in terms of (a) step-down voltage gain; and (b) step-down current gain*

Using volt-second balance principle on inductor L_3, we arrive at the following equation.

$$\frac{V_{CM}}{V_H} = D_b \tag{8}$$

Combining equations (7) and (8), the overall step-down gain for the proposed converter is obtained.

$$\frac{V_L}{V_H} = \frac{{D_b}^2}{2} \tag{9}$$

It is evident from equation (9) that the proposed converter is quadratic in nature. Likewise, the current gain of this converter is given.

$$\frac{I_L}{I_H} = \frac{2}{{D_b}^2} \tag{10}$$

In the above expression, I_L and I_H refer to the load and supply side currents respectively. Fig. 4 compares the step-down voltage and current gains of the proposed converter with respect to other reported works. We can see from the figure that for duty cycles below 0.5, the presented converter has the highest current gain and lowest voltage gain.

3. Control Technique

High current – or high step-down gain – DC-DC converters prove to be an attractive solution for battery charging applications, for a given maximum battery charging current. However, the chosen converter must be complemented by an appropriate charging control scheme to ensure a safe charging process for both the battery and hence, the user.

Consequently, the popular constant current/constant voltage (CC-CV) control strategy is selected for the given topology for battery charging applications. A typical charging current and battery voltage variation as per this control is shown in Fig. 5. The current is held constant till the maximum voltage of the battery is attained. Beyond this point, the current decreases, and the voltage remains constant.

The CV stage is essential as it prevents the battery from overcharging. The CC/CV control technique has proved popular among researchers mainly due to its ease of implementation. Fig. 6(a) shows the CC/CV control scheme block diagram and Fig. 6(b) shows the flowchart for the same. The control scheme block diagram shows that there are two control loop – one each for voltage and current. As long as the battery terminal voltage is below it's maximum value V_{ref}, the current control loop helps regulate the charging current to reference value I_{ref}. Upon reaching V_{ref}, the voltage control loop comes into play, which helps regulate the battery terminal voltage to V_{ref},

Int. Journal of Integrated Engineering Vol. 16 No. 7 (2024) p. 72-82

and the charging current starts to decay. In this scheme, both control loops utilized PI controller, whose outputs were in turn used to determine the switching pulses for all switches.

Using this control technique, quantitative research methods are applied, wherein the battery charging current, battery voltage and state of charge (SoC) were observed over a specific time as shown in subsequent sections. Fig. 7 shows the block diagram of the overall system as seen in MATLAB Simulink.

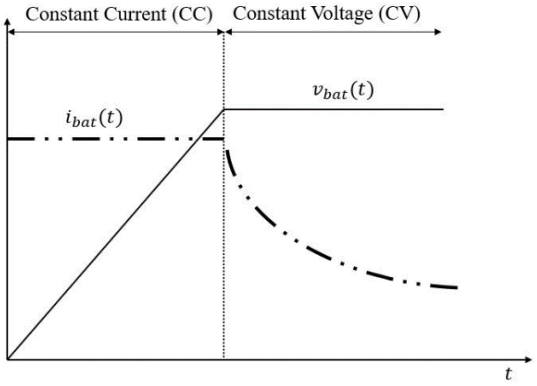

Fig. 5 *Variation of charging current $i_{bat}(t)$ and battery voltage $v_{bat}(t)$ in the CC and CV stages*

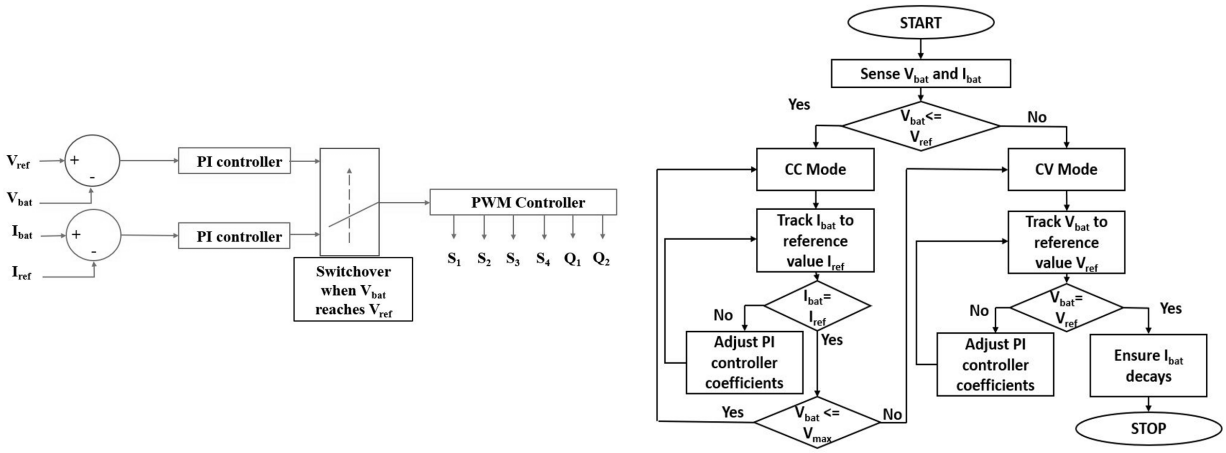

(a) **(b)**

Fig. 6 *(a) Control block diagram for CC-CV strategy; (b) Flowchart for the control process*

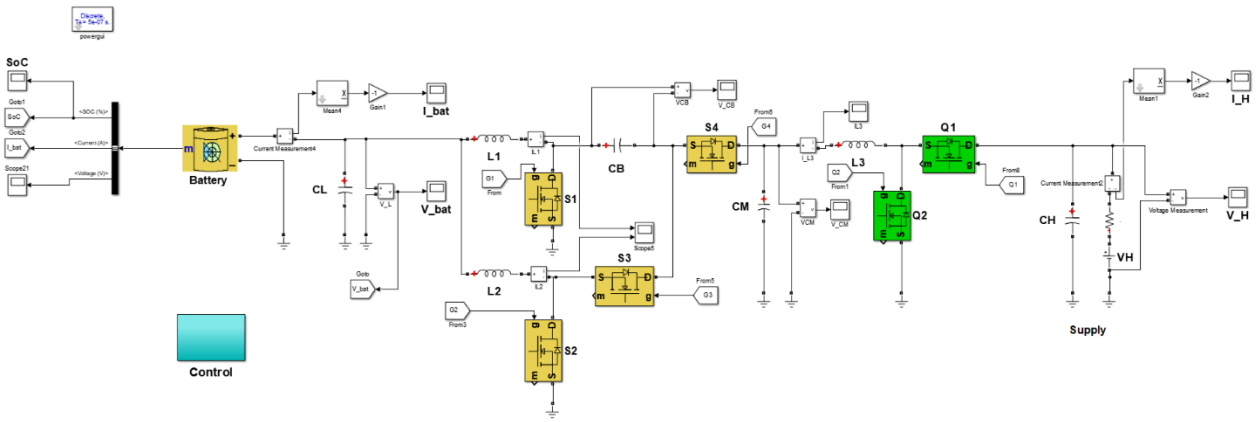

Fig. 7 *Simulation block diagram of the proposed system*

4. Simulation Results and Discussion

Simulation studies were carried out on MATLAB Simulink, using the SImPowerSystems toolbox. Through fine-tuning of converter parameter values in open-loop operation, the final values were chosen as described in Table 1. The battery chosen for this simulation was a 24 V, 10 A h Li-ion battery. The battery charging current reference is set at 10 A, and the battery maximum voltage is 27.93 V – which is its set point. As a consequence of the supply voltage being 300 V, the switch duty cycle D_b is set by the controller at approximately 0.4.

The following parameters were monitored during the simulations: (a) the average battery charging current (b) the average battery terminal voltage and (c) the battery state of charge (SoC). The variations of these parameters over time were observed with respect to time during the CC stage and at the instant of transition from CC to CV mode. Fig. 8 shows the variation of the listed parameters in CC mode. It is observed that owing to controller action, the average charging current is held at the 10 A reference value. Moreover, an upward trend is observed in the average battery terminal voltage – increasing from an initial value of approximately 26 V. The same trend is observed in the SoC, which increases from an initial value of approximately 37.96%. Finally, 93.3% charging efficiency is observed, which is good for the power level at which the converter is operating.

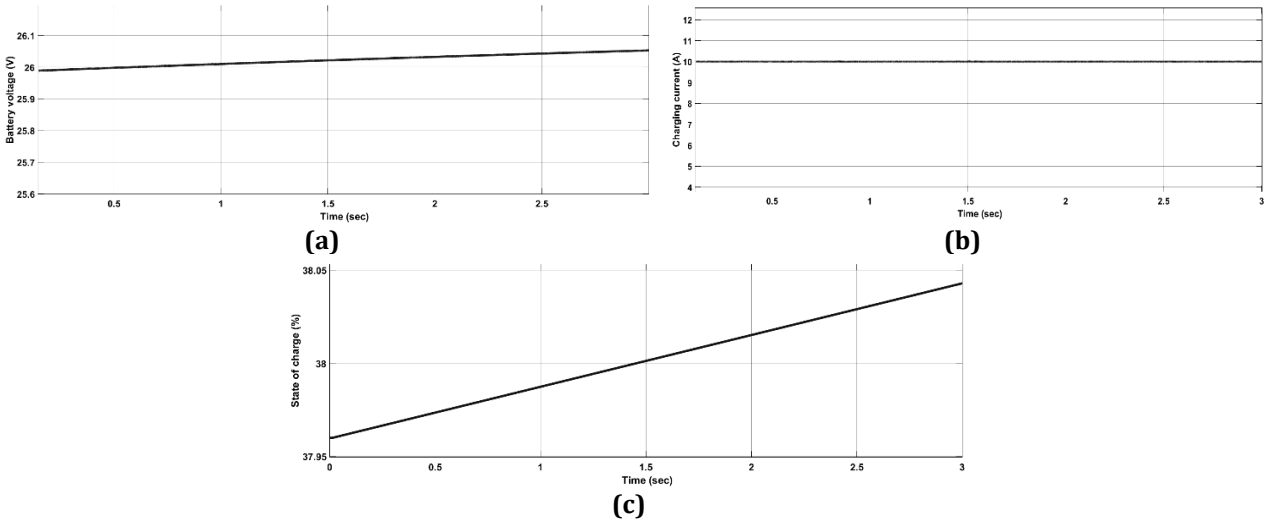

Fig. 8 *Variation of (a) average battery voltage; (b) average charging current; and (c) battery state of charge during CC mode*

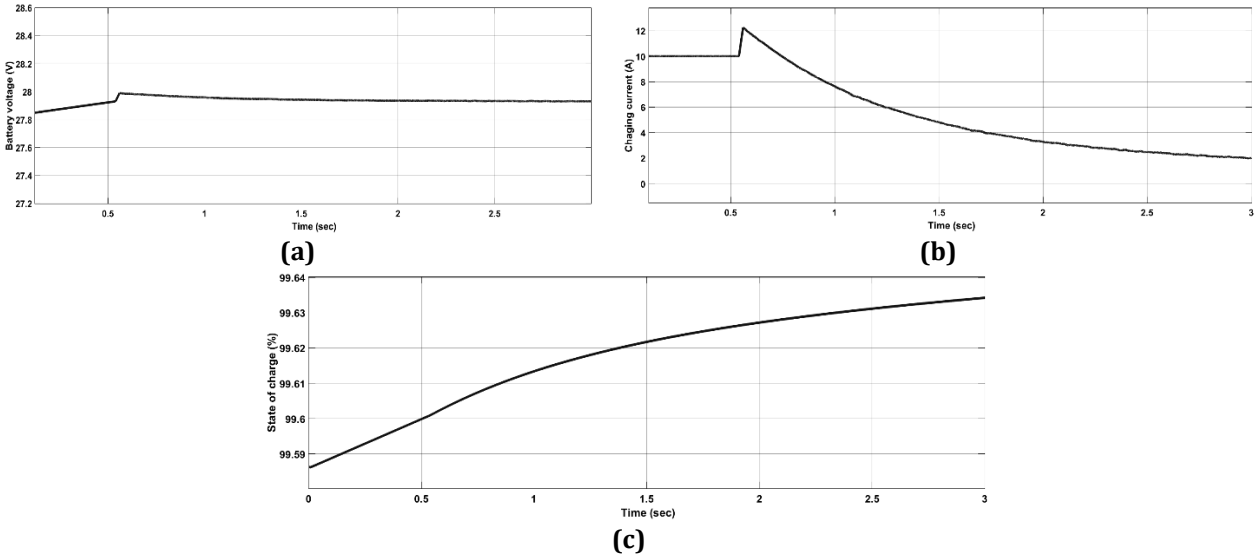

Fig. 9 *Variation of (a) average battery voltage; (b) average charging current; and (c) battery state of charge during CV mode*

The converter control switches over to CV mode once the battery terminal voltage set point of 27.93 V is attained. In this mode, the average charging current starts to reduce from the 10 A set value as seen in Fig. 9. As

Int. Journal of Integrated Engineering Vol. 16 No. 7 (2024) p. 72-82

expected, the controller action ensures that the battery terminal voltage is maintained at the 27.93 V set point, and it is also seen in Fig. 9. One point to note here is the small transient of approximately 0.05 V and 2 A in the terminal voltage and charging current respectively. This occurs as a result of the changeover action of the controller from the CC to CV mode. Lastly, the SoC variation shows that due to the reducing current and the constant voltage, the slope of its increase has also reduced.

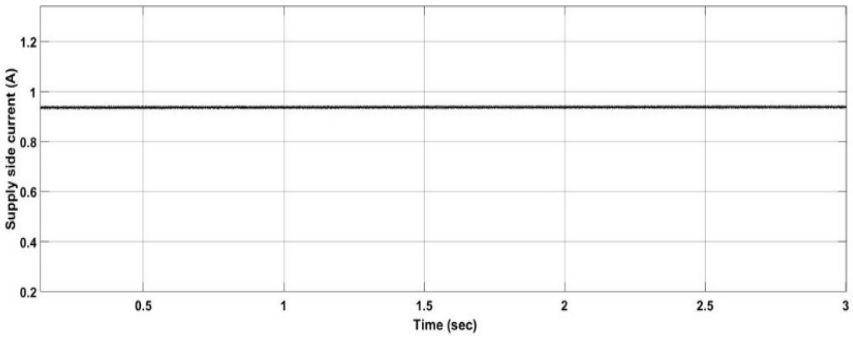

Fig. 10 *Supply side current during CC mode*

The simulation results show that the controller ensures that the battery current and variations follow a typical CC/CV trend as shown in Fig. 5.

Lastly, the high current gain operation of the given converter can also be verified. Fig. 10 shows the supply side current when the converter operates in CC mode. With a value of around 0.9 A, it is validated that the converter is operating with a theoretical gain which corresponds to a duty cycle of approximately 0.4 – which is the approximate output of the controller.

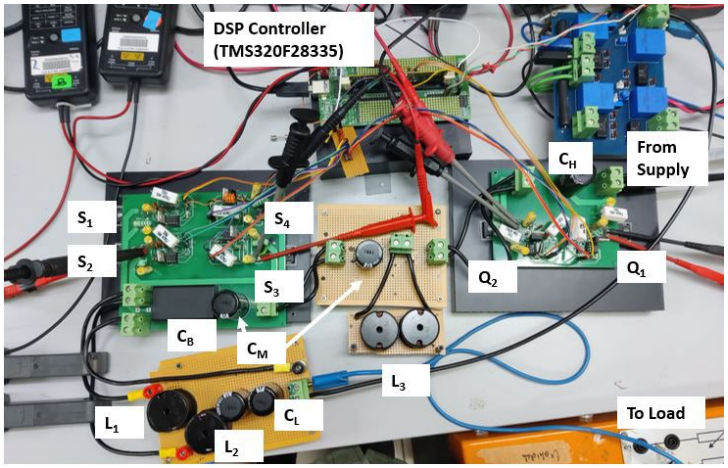

Fig. 11 *Experimental prototype of the given converter*

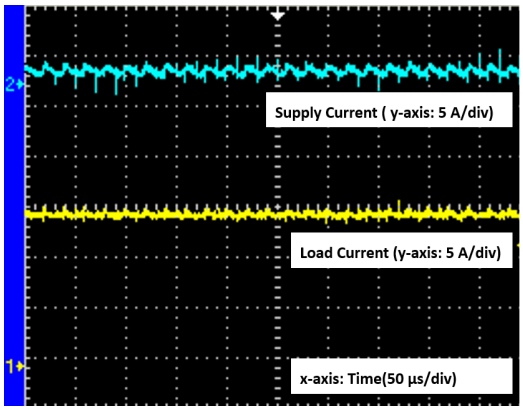

Fig. 12 *Waveforms showing the supply and load currents, obtained from the experimental prototype. Load current is shown in yellow (origin marked as 1) and the supply current is shown in blue (origin marked as 2)*

To further corroborate the high current gain nature of the proposed converter, a prototype was built wherein the components of the same values as in Table 1 were chosen – with the overall layout of the prototype as shown in Fig. 11. Cree C3M0065100K SiC MOSFETs were used as switches in the converter, mainly because of their superior switching characteristics over a conventional MOSFET. The converter was operated in an open loop condition with a 1.8 Ω resistive load, and the duty cycle of the switch operation was fixed at 0.4. As shown in Fig. 12, the load current (in yellow) was observed to be approximately 15 A, while the input current (in blue) was observed to be approximately 1.32 A. Using these values, a current gain of approximately 11.36 was observed. Theoretically, if the duty cycle D_b of 0.4 is chosen and it is used in equation (10), the current gain is calculated to be 12.5, which can also be derived from the current gain plot shown in Fig. 4(a). Hence, the observed and theoretical value of the current gain are observed to be close to each other. Going back to Fig. 4, the superior current gain of the proposed converter over other contemporary reported works is also validated. Hence, the high current gain nature of the proposed converter is verified, and it can be used in high current applications.

4.1 Conclusion

A cascaded DC-DC converter – which combined a synchronous buck converter and a series capacitor synchronous buck converter – was presented in this paper. This converter was then evaluated for battery charging applications in a MATLAB Simulink environment. For this purpose, a 24 V 10 A h Li-ion battery was chosen.

A charging current of 10 A was maintained due to controller action in the CC stage, which resulted in a steady increase in battery terminal voltage and SoC. This process continued until the reference voltage – which was the maximum battery voltage in this case – was attained. This marked the start of the CV mode, and beyond this point, the controller action helped hold the battery voltage constant, which led to a steady decrease in the charging current from its 10 A set point. The SoC's slope of increase also reduced in this stage. Additionally, the control changeover resulted in a small transient in the battery voltage and charging current at the start of CV mode. This transient was kept to a minimum by tuning of PI controller parameters.

Significantly, a satisfactory 93.3% charging efficiency was observed, which is good for the power level at which the converter operated, thus validating the topology's usage in charging applications.

Another significant result from the simulations is the verification of the high current gain operation of the given topology. The battery charging current of 10 a roughly translated to a supply side current of 0.9 A. This corresponds to the theoretical gain at a duty cycle of approximately 0.4. This indicates the straightforward nature of cascading converters to achieve a high step-down gain or current gain, and it can be used for other applications which require the same. This aspect of the converter was further validated through hardware experimentation, wherein the circuit was run in open loop with a 1.8 Ω resistive load. It was observed that the theoretical and the experimental value of the current gain were found to be close, thus proving its suitability for high current applications.

The simulation results and resultant charging efficiency indicate the suitability of this converter for battery charging. This converter can potentially be scaled up for battery packs with higher voltage ratings – those which may be found in electric two/three-wheelers. This work aims to address the need for coverage expansion of LEVs through improvements in charging infrastructure, with emphasis on off-board charging for electric three-wheelers suited for public transportation. In this regard. This can also help alleviate any possible issue of vehicle battery discharge during peak operating hours. Further validation may be done through hardware implementation and real-time operation of the proposed DC-DC converter topology to gauge the suitability of the given converter for a higher battery rating and evaluate the charging time.

Acknowledgement

The work is supported financially by the Ministry of Higher Education Malaysia via Fundamental Research Grant Scheme (FRGS/1/2020/TK0/UM/02/41).

Conflict of Interest

Authors declare that there is no conflict of interests regarding the publication of the paper.

Author Contribution

The authors confirm contribution to the paper as follows: ***study conception and design:*** *Mohammad Faisal Akhtar, Siti Rohani Sheikh Raihan, Nasrudin Abdul Rahim;* ***data collection:*** *Mohammad Faisal Akhtar;* ***analysis and interpretation of results:*** *Mohammad Faisal Akhtar, Siti Rohani Sheikh Raihan;* ***draft manuscript preparation:*** *Mohammad Faisal Akhtar, Siti Rohani Sheikh Raihan, Mohd Khairil Rahmat. All authors reviewed the results and approved the final version of the manuscript.*

References

[1] International Energy Agency. Global EV Outlook 2022; IEA: Paris, France, 2022.
[2] Sasidharan, C.; Tyagi, B.; Rajah, V. Light electric vehicles and their charging aspects. In Electric Vehicles; Springer: Singapore, 2021; pp. 33–51.

[3] Mouli, G.R.C.; van Duijsen, P.; Grazian, F.; Jamodkar, A.; Bauer, P.; Isabella, O. Sustainable e-bike charging station that enables ac, dc and wireless charging from solar energy. Energies 2020, 13, 3549.
[4] Singh, B.; Gupta, J. Improved Power Quality On-Board Charging Solution for Light Electric Vehicles. In Proceedings of the 2021 IEEE Transportation Electrification Conference & Expo (ITEC), Chicago, IL, USA, 21–25 June 2021; pp. 462–467.
[5] Rafi, M.A.H.; Bauman, J. A Comprehensive Review of DC Fast-Charging Stations with Energy Storage: Architectures, Power Converters, and Analysis. IEEE Trans. Transp. Electrif. 2021, 7, 345–368.
[6] Sabzali, A. J., Ismail, E. H., Al-Saffar, M. A., and Behbehani, H. M. (2015) Non-isolated single-switch DC–DC converters with extended duty cycle for high step-down voltage applications. Int. J. Circ. Theor. Appl., 43: 1080– 1094. doi: 10.1002/cta.2000.
[7] Rajesh, P., Shajin, F.H. & Kommula, B.N. An efficient integration and control approach to increase the conversion efficiency of high-current low-voltage DC/DC converter. Energy Syst 13, 939–958 (2022). https://doi.org/10.1007/s12667-021-00452-w
[8] Yu, M., Sha, D. and Liao, X. (2014), Hybrid phase shifted full bridge and LLC half bridge DC–DC converter for low-voltage and high-current output applications. IET Power Electronics, 7: 1832-1840. https://doi.org/10.1049/iet-pel.2013.0778
[9] Lai, C.-M. Development of a Novel Bidirectional DC/DC Converter Topology with High Voltage Conversion Ratio for Electric Vehicles and DC-Microgrids. Energies 2016, 9, 410.
[10] Y. Zheng, S. Li and K. M. Smedley, "Nonisolated High Step-Down Converter With ZVS and Low Current Ripples," in IEEE Transactions on Industrial Electronics, vol. 66, no. 2, pp. 1068-1079, Feb. 2019, doi: 10.1109/TIE.2018.2833047.
[11] H. Moradisizkoohi, N. Elsayad and O. A. Mohammed, "A Voltage-Quadrupler Interleaved Bidirectional DC–DC Converter With Intrinsic Equal Current Sharing Characteristic for Electric Vehicles," in IEEE Transactions on Industrial Electronics, vol. 68, no. 2, pp. 1803-1813, Feb. 2021, doi: 10.1109/TIE.2020.2998757.
[12] R. Mayer, M. B. E. Kattel and S. V. G. Oliveira, "Multiphase Interleaved Bidirectional DC/DC Converter With Coupled Inductor for Electrified-Vehicle Applications," in IEEE Transactions on Power Electronics, vol. 36, no. 3, pp. 2533-2547, March 2021, doi: 10.1109/TPEL.2020.3015390.
[13] J. Chen, D. Sha, Y. Yan, B. Liu and X. Liao, "Cascaded High Voltage Conversion Ratio Bidirectional Nonisolated DC–DC Converter With Variable Switching Frequency," in IEEE Transactions on Power Electronics, vol. 33, no. 2, pp. 1399-1409, Feb. 2018, doi: 10.1109/TPEL.2017.2679105.
[14] S. H. Hosseini, R. Ghazi and H. Heydari-Doostabad, "An Extendable Quadratic Bidirectional DC–DC Converter for V2G and G2V Applications," in IEEE Transactions on Industrial Electronics, vol. 68, no. 6, pp. 4859-4869, June 2021, doi: 10.1109/TIE.2020.2992967.
[15] A. R. N. Akhormeh, K. Abbaszadeh, M. Moradzadeh and A. Shahirinia, "High-Gain Bidirectional Quadratic DC–DC Converter Based on Coupled Inductor With Current Ripple Reduction Capability," in IEEE Transactions on Industrial Electronics, vol. 68, no. 9, pp. 7826-7837, Sept. 2021, doi: 10.1109/TIE.2020.3013551.
[16] C.-M. Lai, Y.-H. Li, Y.-H. Cheng, and J. Teh, “A High-Gain Reflex-Based Bidirectional DC Charger with Efficient Energy Recycling for Low-Voltage Battery Charging-Discharging Power Control,” Energies, vol. 11, no. 3, p. 623, Mar. 2018, doi: 10.3390/en11030623.
[17] S. Dusmez, A. Cook and A. Khaligh, "Comprehensive analysis of high quality power converters for level 3 off-board chargers," 2011 IEEE Vehicle Power and Propulsion Conference, Chicago, IL, USA, 2011, pp. 1-10, doi: 10.1109/VPPC.2011.6043096.
[18] Nowakowski, R., & Tang, N. (2009). Efficiency of synchronous versus nonsynchronous buck converters. Texas Instruments Incorporated.
[19] Semiconductor, O. N. (2013). LC selection guide for the DC-DC synchronous buck converter. AND9135/D.
[20] Ahmed Rmila, S., & Ang, S. S. (2020). A High-Input Voltage Two-Phase Series-Capacitor DC-DC Buck Converter. Journal of Electrical and Computer Engineering, 2020, 1-15.